

# Microstructure and mechanical properties of gas pressure sintered $\text{Al}_2\text{O}_3/\text{TiCN}$ composite

Haitao Yang<sup>a,1,\*</sup>, Fuliang Shang<sup>b</sup>, Ling Gao<sup>a</sup>

<sup>a</sup> Shenzhen Key Lab of Special Functional Materials, Department of Materials, School of Science, Shenzhen University, Shenzhen 518060, Guangdong, PR China

<sup>b</sup> State Key Lab of Advanced Technology for Materials Synthesis and Processing, Wuhan University of Technology, Wuhan 430070, China

Received 5 April 2006; received in revised form 21 April 2006; accepted 2 July 2006

Available online 15 September 2006

## Abstract

$\text{Al}_2\text{O}_3$ –30 wt.%TiCN composites have been fabricated successfully by a two-stage gas pressure sintering schedule. The gas pressure sintered  $\text{Al}_2\text{O}_3$ –30 wt.%TiCN composite achieved a relative density of 99.5%, a bending strength of 772 MPa, a hardness of 19.6 GPa, and a fracture toughness of  $5.82 \text{ MPa m}^{1/2}$ . The fabrication procedure involves solid state sintering of two phases without solubility to prepare  $\text{Al}_2\text{O}_3$ –TiCN composite. Little grain growth occurred for TiCN during sintering while  $\text{Al}_2\text{O}_3$  grains grew about three times to an average size of 3–5  $\mu\text{m}$ . The interface microstress arising during cooling from the processing temperature because of the thermal and/or mechanical properties mismatch between the  $\text{Al}_2\text{O}_3$  and TiCN phase is about 50 MPa. Such a compressive microstress is not high enough to cause grain boundary cracking that may weaken the composite but it can introduce dislocations within grains, which is very good to enhance the composite properties.

© 2006 Elsevier Ltd and Techna Group S.r.l. All rights reserved.

**Keywords:** C. Mechanical properties; D.  $\text{Al}_2\text{O}_3$ ; Gas pressure sintering; Microstructure

## 1. Introduction

The  $\text{Al}_2\text{O}_3/\text{TiC}$  composites consist of small titanium carbide grains dispersed in an alumina matrix and have been widely used for high speed cutting of hard steel, superalloys, or cast iron [1–4]. The characterization of their mechanical properties has also been an interesting subject for research because of the possible toughening effects resulting from the thermal and/or mechanical properties mismatch between of the  $\text{Al}_2\text{O}_3$  and TiC phases [5,6]. Hot pressing is commonly used to prepare  $\text{Al}_2\text{O}_3/\text{TiC}$  composite, which has many limitations for mass production. Gas-pressure sintering is now widely used to fabricate high-performance ceramics with complex shapes because of its economic advantages over hot isostatic pressing (HIP) and improvements in relative density and mechanical properties compared to those produced by pressureless sintering [7,8]. TiCN is now very attractive in applications as cutting tools due to its superior mechanical and tribological

properties (e.g. lower friction coefficient) compared to traditional TiC and TiN [9,10]. Based on these observations, the microstructure and the densification behavior as well as the mechanical properties of the gas pressure sintered  $\text{Al}_2\text{O}_3/\text{TiCN}$  composite were investigated in the present study.

## 2. Experimental

The alumina powder used in the present study had a purity of 99.5%, a mean particle size of 1  $\mu\text{m}$ , and a  $\alpha$ -phase of above 90%.  $\text{TiC}_{0.7}\text{N}_{0.3}$  (Beijing Non-ferrous Institute, China, 99% purity, 1  $\mu\text{m}$ ) was used as an additive. The powder mixtures were prepared in 200 g batches consisting of 70 wt.%  $\text{Al}_2\text{O}_3$  and 30 wt.%TiCN. Each powder batch was mixed and ball milled in alcohol for 24 h with alumina medium. The powder mixtures were dry-pressed into bars in a steel die at 100 MPa. The green compacts were sintered in a graphite crucible in a graphite furnace capable of operating at temperatures of up to 2000 °C in an inert atmosphere of up to 10 MPa pressure. A two-stage sintering schedule was utilized in the present study, which included a first stage at a sintering temperature of 1700–1850 °C for 30 min under a low argon gas pressure of 0.2–0.5 MPa and a second stage at the same

\* Corresponding author.

E-mail address: [yanght63@hotmail.com](mailto:yanght63@hotmail.com) (H. Yang).

<sup>1</sup> Visiting scientist at Department of Materials, University of Oxford (March 2003 to March 2004).

temperature for 60 min under a high pressure of 6–8 MPa. The heating and cooling rates were 10 °C/min. The high argon gas pressure was maintained during cooling until the temperature was below 1200 °C.

The bulk density was measured using the Archimedeian principle. Without being ground and polished, the sintered bar specimens, 5 mm × 5 mm × 30 mm in size, were used directly for three-point bending strength measurements at a crosshead speed of 0.5 mm/min, with a bottom span of 24 mm. Ten samples were used for each strength data point. The fracture toughness was measured by the indentation method according to Ref. [11]. The surface was polished for Vickers indentation, and a load of 49 N was used for 15 s to induce indentations. Three data points were measured for each sample and five samples were used for each fracture toughness data point. The TEM samples were prepared as follows. Slices of materials ~1000 μm thick were cut from the sintered bars, ground on a diamond wheel to ~200 μm thickness, and then polished to ~120 μm thickness using 6 μm diamond paste. Discs with a diameter of 3 mm were cut from the polished slices using a supersonic drill with water and silicon carbide grinding medium. A Gatan dimple grinder was used to polish each side using 1 μm diamond, leaving a central area ~20 μm thickness. Finally the dimpled region was thinned to electron transparency using a Precision Ion Polishing System (Gatan 600, USA). A transmission electron microscopy (JEOL 200CX) was used to observe the microstructures. In order to prevent charging during observation, the specimens were coated with carbon prior to observation.

### 3. Results and discussion

The reason that the two stage sintering schedule was used is that the bulk density greater than 92% was achieved in the first stage of sintering under low pressure and then nearly full density could be achieved in the second stage of sintering under high pressure of 6–8 MPa argon which is about 5% of the pressure of HIP.

The relative density and the mechanical properties of the Al<sub>2</sub>O<sub>3</sub>–30 wt.%TiCN composite gas pressure sintered at different temperatures are listed in Table 1.

The optimal sintering temperature is at 1800 °C, which corresponds to the highest relative density of 99.5%, the highest bending strength of 772 MPa, the highest toughness of 5.85 MPa m<sup>1/2</sup> and the highest hardness of 19.6 GPa. It is reasonable that the higher the relative density, the higher the mechanical properties for ceramic materials.

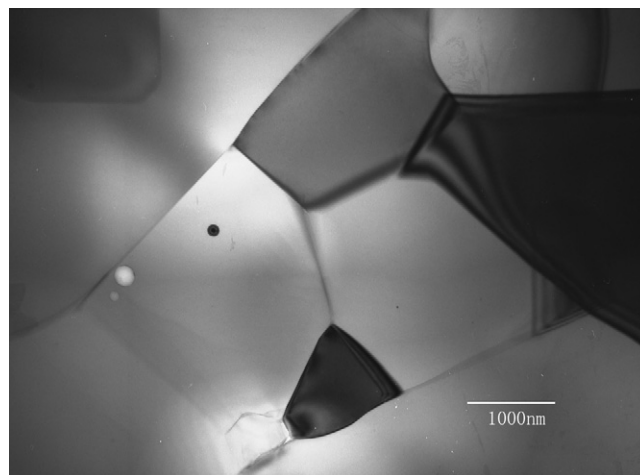


Fig. 1. Typical TEM micrograph of the Al<sub>2</sub>O<sub>3</sub>–30 wt.%TiCN composite gas pressure sintered at 1800 °C.

Now alumina ceramics with a flexural strength of above 700 MPa and a fracture toughness of above 4 MPa m<sup>1/2</sup> have been prepared by using pure and fine powder [12]. Considering its relative density and the mechanical properties as well as the particle size of the raw alumina powders, the gas pressure sintered Al<sub>2</sub>O<sub>3</sub>–30 wt.%TiCN composite in the present study is very successful.

A typical TEM micrograph of the Al<sub>2</sub>O<sub>3</sub>–30 wt.%TiCN composite sintered at 1800 °C is shown in Fig. 1. The large bright grains sized 3–5 μm are Al<sub>2</sub>O<sub>3</sub> grains. The small dark TiCN grains sized about 1 μm were distributed homogeneously at grain junctions in Al<sub>2</sub>O<sub>3</sub> matrix. Considering the particle size of ~1 μm of the Al<sub>2</sub>O<sub>3</sub> powder used in the present study, Al<sub>2</sub>O<sub>3</sub> grains grew about three times during sintering. It was observed that some very small TiCN particles in nanometer scale are dispersed in Al<sub>2</sub>O<sub>3</sub> grains (Fig. 2). Because there is no reported solubility of TiC, TiN, or TiC<sub>x</sub>N<sub>1–x</sub> in Al<sub>2</sub>O<sub>3</sub> in the literature and one would not expect any solubility, the TiCN particles found within Al<sub>2</sub>O<sub>3</sub> grains should therefore be the result of grain growth of alumina. The melting point of TiC and Al<sub>2</sub>O<sub>3</sub> is about 3147 and 2050 °C, respectively, so when sintered at 1800 °C, it is a typical solid state sintering of two phases without solubility. Very little grain growth occurred during sintering for TiCN. Although the average particle size of TiCN before sintering is about 1 μm, there is a distribution of sizes, with some particles being smaller than 100 nm. Actually the TiCN particles remained almost unchanged during sintering of the Al<sub>2</sub>O<sub>3</sub>/TiN nanocomposite just as Todd and co-workers

Table 1

The relative density and the mechanical properties of the Al<sub>2</sub>O<sub>3</sub>–30 wt.%TiCN composite gas pressure sintered at different temperatures

Sintering temperature (°C)	Relative density (%)	Bending strength (MPa)	Toughness (MPa m <sup>1/2</sup> )	Hardness (GPa)
1700	97.2 ± 0.6	643 ± 80	5.45 ± 0.2	18.6 ± 1.2
1750	98.3 ± 0.2	685 ± 56	5.65 ± 0.2	19.2 ± 1.3
1800	99.5 ± 0.3	772 ± 78	5.85 ± 0.1	19.6 ± 1.5
1850	99.0 ± 0.5	700 ± 72	5.72 ± 0.2	19.4 ± 1.2

Theoretical density = 4.28 g/cm<sup>3</sup> for Al<sub>2</sub>O<sub>3</sub>–30 wt.%TiCN.

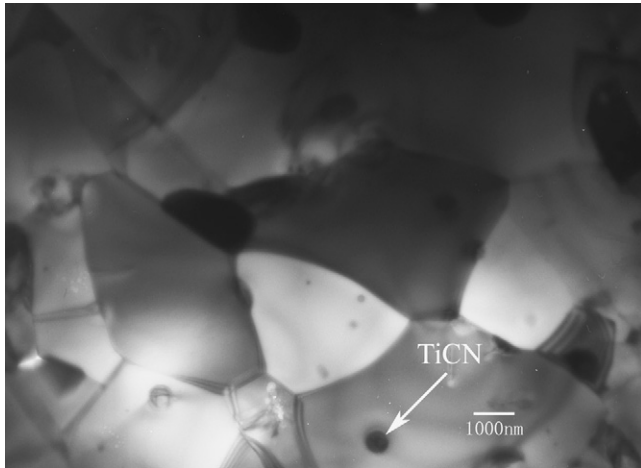


Fig. 2. TEM photograph showing small TiCN particles in nanometer scale dispersed in  $\text{Al}_2\text{O}_3$  grains.

[13,14] found in their study that the nano SiC particles were almost unchanged in the sintering of  $\text{Al}_2\text{O}_3/\text{SiC}$  nanocomposite. The transgranular fracture is predominant for the  $\text{Al}_2\text{O}_3$ –30 wt.%TiCN composite sintered at 1800 °C, which is usually the characteristic of high fracture strength. Fig. 3 shows microcracks propagated through the grains and the crack propagation was stopped by a TiCN particle.

The mechanical properties of pure alumina have been improved by adding TiC, TiN, or  $\text{TiC}_x\text{N}_{1-x}$  to form particle-reinforced ceramic composites by the following mechanisms. First, the matrix transfers some of the applied stress to the particles, which bear a fraction of the load; second, these reinforcing particles tend to impede the grain growth of the alumina matrix phase; third, the cracks are deflected by these reinforcing particles; and fourth, some toughening results from the thermal and/or mechanical properties mismatch between the  $\text{Al}_2\text{O}_3$  and TiCN phases. The compressive residual stresses arise during cooling from processing temperatures due to the thermal and/or mechanical properties mismatch between the  $\text{Al}_2\text{O}_3$  and TiCN phases [14].

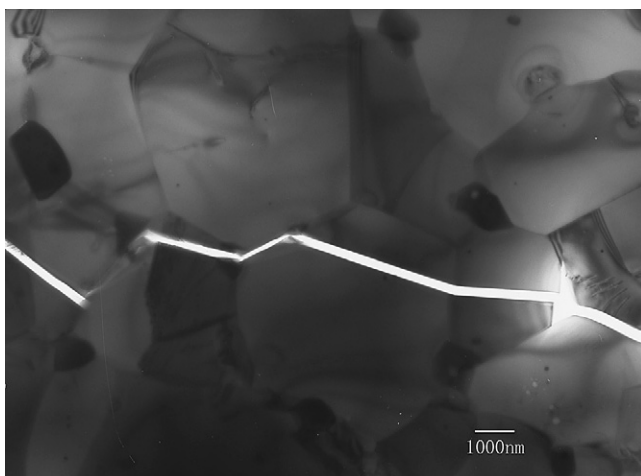


Fig. 3. TEM photograph showing microcracks propagating through the grains and the crack arrest by a TiCN particle.

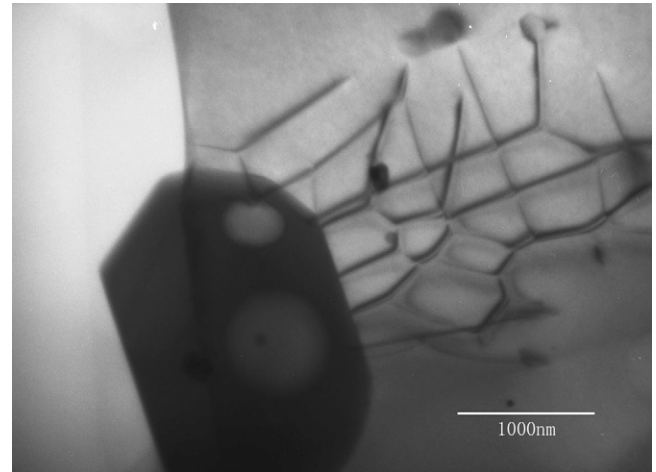


Fig. 4. TEM photograph illustrating the dislocations in strong diffraction contrast in an  $\text{Al}_2\text{O}_3$  grain where a big TiCN particle is located nearby.

The residual stress in the fine-grained  $\text{TiC}_x\text{N}_{1-x}$  composites in the present study is estimated by the equation [15]

$$\sigma_i = K(\alpha_r - \alpha_i)\Delta T \quad (1)$$

where  $\alpha_r$  and  $\alpha_i$  are the average volume expansion coefficient and volume expansion coefficient for particle  $i$ ,  $\Delta T$  the temperature change from the stress-free state, and  $K$  is the bulk modulus ( $K = E/3(1 - 2\mu)$ , where  $E$  is the elastic modulus, and  $\mu$  the Poisson's ratio). For the  $\text{Al}_2\text{O}_3/\text{TiCN}$  system, the linear expansion coefficients of  $\text{Al}_2\text{O}_3$  and TiCN are  $8.24 \times 10^{-6}$  and  $8.35 \times 10^{-6}$ , respectively [12], with the average value estimated to be about  $8.30 \times 10^{-6}$ , and since volume expansion coefficient equals approximately three times linear expansion coefficient, the parameter  $(\alpha_r - \alpha_i)$  is about  $0.2 \times 10^{-6}$ . The elastic modulus of  $\text{Al}_2\text{O}_3$  and TiCN are  $380 \times 10^3$  and  $400 \times 10^3$  MPa, respectively, with an average value estimated to be about  $390 \times 10^3$  MPa,  $\mu$  is about 0.25, and  $\Delta T$  is about  $2 \times 10^3$  K, the sintering temperature. According to Eq. (1), the residual stress on each particle  $\sigma_i$  is about 50 MPa. Such a compressive microstress is not high enough to cause grain boundary cracking that may weaken the composite but it may introduce dislocations within grains, which is very good to enhance the composites properties. That explains the very good mechanical properties of the  $\text{Al}_2\text{O}_3$ –TiCN composite in the present study. Fig. 4 illustrates the dislocations under strong diffraction contrast in an  $\text{Al}_2\text{O}_3$  grain where a big TiCN particle is located nearby.

#### 4. Conclusions

$\text{Al}_2\text{O}_3$ –30 wt.%TiCN composite have been fabricated successfully by a two stage gas pressure sintering schedule. The gas pressure sintered  $\text{Al}_2\text{O}_3$ –30 wt.%TiCN composite achieved a relative density of 99.5%, a bending strength of 772 MPa, a hardness of 19.6 GPa, and a fracture toughness of  $5.82 \text{ MPa m}^{1/2}$ .

The fabrication procedure involves solid state sintering of two phases without solubility to form the  $\text{Al}_2\text{O}_3$ –TiCN composite. Little grain growth occurred for TiCN during sintering while  $\text{Al}_2\text{O}_3$  grains grew about three times to 3–5  $\mu\text{m}$ . The interface microstress arising during cooling from the processing

temperature because of the thermal expansion mismatch between the  $\text{Al}_2\text{O}_3$  and TiCN phases is about 50 MPa. Such a compressive microstress is not high enough to cause grain boundary cracking that may weaken the composite but is high enough to introduce dislocations within grains, which is very good to enhance the composites properties.

### Acknowledgements

This work was supported by State Ministry of Education of the PR China under the contract No. 02049 as well as by the National Science Foundation under the Grant No. 50220160657 for International Cooperation. We are grateful to the Department of Materials, University of Oxford for the use of their EM facilities.

### References

- [1] M. Masuda, T. Sato, T. Kori, Y. Chujo, Cutting performance and wear mechanism of alumina-based ceramic tools when machining austempered ductile iron, *Wear* 174 (1992) 147–153.
- [2] T. Takahashi, Development of fine and high-strength  $\text{Al}_2\text{O}_3$  based ceramics, *J. Jpn. Soc. Powder Powder Metall.* 45 (1998) 496–506.
- [3] G. Jianghong, Z. Zhe, Y. Yang, G. Zhenduo, M. Hezhuo, Statistical variability in the indentation toughness of TiCN particle reinforced  $\text{Al}_2\text{O}_3$  composite, *Mater. Lett.* 49 (2001) 357–360.
- [4] A. Goldstein, A. Singurindi,  $\text{Al}_2\text{O}_3/\text{TiC}$  based metal cutting tools by microwave sintering followed by hot isostatic pressing, *J. Am. Ceram. Soc.* 83 (6) (2000) 530–532.
- [5] M. Furukawa, O. Nakano, Y. Takashima, Fracture toughness of  $\text{Al}_2\text{O}_3$ –TiC ceramics, *Int. J. Refrac. Hard Metals* 7 (1988) 37–40.
- [6] N. Tamari, T. Tanaka, I. Kondoh, K. Tezuka, T. Yamamoto, Mechanical properties and cutting performance of titanium carbide whisker/alumina composites, *J. Ceram. Soc. Jpn.* 104 (1996) 439–444.
- [7] K.B. Sampad, L.R. Frank, Gas pressure sintering of silicon nitride powder coated with  $\text{Al}_2\text{O}_3$  and  $\text{TiO}_2$ , *J. Am. Ceram. Soc.* 86 (2) (2003) 212–216.
- [8] S.-J. Cho, K.-J. Yoon, Nonuniform densification during gas pressure sintering of an sialon ceramic, *J. Am. Ceram. Soc.* 81 (9) (1998) 2458–2460.
- [9] D. Mari, S. Bolognini, T. Viatte, W. Benoit, Study of the mechanical properties of TiCN–WC–Co hardmetals by the interpretation of internal friction spectra, *Int. J. Refrac. Metals Hard Mater.* 19 (4–6) (2001) 257–265.
- [10] K.J. Ma, C.L. Chao, D.S. Liu, Y.T. Chen, M.B. Shieh, Friction and wear behavior of TiN/Au, TiN/MoS<sub>2</sub> and TiN/TiCN/a-C:H coatings, *J. Mater. Process. Technol.* 127 (2) (2002) 182–186.
- [11] G.R. Antsis, P. Chantikul, B.R. Lawn, D.B. Marshall, A critical evaluation of indentation techniques for measuring fracture toughness. 1. Direct crack measurements, *J. Am. Ceram. Soc.* 64 (9) (1981) 533–538.
- [12] X. Li, Z. Ziu, X. Sun, L. Zheng, Preparation of  $\text{Al}_2\text{O}_3/\text{TiCN}$  composites by normal pressure sintering, *Guisuanyan Zuebao* 31 (11) (2003) 1069–1074 (in Chinese).
- [13] C.N. Walker, C.E. Borsa, R.I. Todd, et al., Fabrication, characterization and properties of alumina matrix nanocomposites., *Brit. Ceram. Proc.* 53 (1994) 249–264.
- [14] R.I. Todd, M.A. Bourke, C.E. Borsa, R.J. Brook, Neutron diffraction measurements of residual stress in alumina/SiC nanocomposites, *Acta Mater.* 45 (4) (1997) 1791–1800.
- [15] W.D. Kingery, *Introduction to Ceramics*, John Wiley & Sons Inc., 1960, pp. 478.